Subsequently, other groups have applied this protocol to other difficult structure determinations, with similar success; for example, the RecA protein of *E. coli* (Story, Weber & Steitz, 1992) and the engrailed homeodomain/DNA complex (Kissinger, Liu, Martin-Blanco, Kornberg & Pabo, 1990). Other more recent examples and a critical examination of the application of this method is presented by Cura, Krishnaswamy & Podjarny (1992).

While solvent flattening provided the phase constraints for decoupling parent-phase generation from heavy-atom refinement, other sources may be exploited, for example noncrystallographic symmetry (Bricogne, 1976; Cura, Krishnaswamy & Podjarny, 1992), translational noncrystallographic symmetry (Agard & Stroud, 1982) and entropy maximization (Prince, Sjölin & Alenljung, 1988). These and other constraints are reviewed by Tulinsky (1985) and Podjarny, Bhatt & Zwick (1987).

References

AGARD, D. A. & STROUD, R. M. (1982). *Acta Cryst.* A**38**, 186-194.

BHAT, T. N. & BLOW, D. M. (1982). *Acta Cryst.* A**38**, 21-29.

BLOW, D. M. & CRICK, F. H. C. (1959). *Acta Cryst.* **12**, 794-802.

BLOW, D. M. & MATTHEWS, B. W. (1973). *Acta Cryst.* A**29**, 56-62.

BRICOGNE, G. (1976). *Acta Cryst.* A**32**, 832-847.

CURA, V., KRISHNASWAMY, S. & PODJARNY, A. D. (1992). *Acta Cryst.* A**48**, 756-764.

HENDRICKSON, W. A. & LATTMAN, E. E. (1970). *Acta Cryst.* B**26**, 136-143.

KISSINGER, C. R., LIU, B., MARTIN-BLANCO, E., KORNBERG, T. B. & PABO, C. O. (1990). *Cell*, **63**, 579-590.

PODJARNY, A. D., BHATT, T. N. & ZWICK, M. (1987). *Annu. Rev. Biophys. Biophys. Chem.* **16**, 351-373.

PRINCE, E., SJÖLIN, L. & ALENLJUNG, R. (1988). *Acta Cryst.* A**44**, 216-222.

ROULD, M. A., PERONA, J. J., SOLL, D. & STEITZ, T. A. (1989). *Science*, **246**, 1135-1142.

SCHEVITZ, R. W., PODJARNY, A. D., ZWICK, M., HUGHES, J. J. & SIGLER, P. B. (1981). *Acta Cryst.* A**37**, 669-677.

SERC Daresbury Laboratory (1986). *CCP4. A Suite of Programs for Protein Crystallography.* SERC Daresbury Laboratory, Warrington, England.

STEIGEMANN, W. & HUBER, R. (1982). *PROTEIN Crystallographic Program Suite.* Max-Planck Institut für Biochemie, Martinsried, Germany,

STORY, R. M., WEBER, I. T. & STEITZ, T. A. (1992). *Nature (London)*, **335**, 318-325.

TULINSKY, A. (1985). *Methods Enzymol.* **115**, 77-89.

WANG, B. C. (1985). *Methods Enzymol.* **115**, 90-112.

Acta Cryst. (1992). A**48**, 756-764

Heavy-Atom Refinement Against Solvent-Flattened Phases

BY V. CURA, S. KRISHNASWAMY* AND A. D. PODJARNY†

Laboratoire de Cristallographie Biologique, IBMC du CNRS, 15 rue Descartes, 67084 Strasbourg, France

(*Received* 11 *September* 1991; *accepted* 20 *March* 1992)

Abstract

A new algorithm for refinement of heavy-atom parameters is defined by an iterative procedure where external phases are provided by density modification. This algorithm is applied to two cases, $tRNA^{Asp}$ and the complex between $tRNA^{Asp}$ and aspartyl-tRNA synthetase. In the first case, where the structure was solved by multiple isomorphous replacement (MIR) methods, it was found that the new method gives accurate values for the native-derivative scale and for occupancy of heavy-atom sites. Position refinement was more delicate and it needed to be handled in a restricted resolution range. In the second case, where a similar method was used in the early stages of solving the phase problem, it slightly decreased the phase error. It was followed by an improvement of the density-modification masks, which led to better maps at higher resolution.

Introduction

Heavy-atom isomorphous replacement (Blow & Crick, 1959) is widely used for phasing a new molecular structure. However, its application is rarely straightforward (Philips, 1988; Blow, Henrick & Vrielink, 1988) and new developments such as improvements of the error analysis (Read, 1991) or of the underlying theory (Bricogne, 1992; Otwinowski, 1992) are welcome.

The refinement of heavy-atom parameters relies on the proper estimate of either the heavy-atom amplitude or the protein phase. The first option is adequate if enough centric reflections or good-quality derivative anomalous-dispersion data are available. If this is not the case, it is necessary to estimate the protein phase independently of the heavy-atom parameters under refinement (Dodson, 1976, and references

* Present address: Madurai Kamaraj University, Madurai, India.

† To whom correspondence should be addressed.

0108-7673/92/050756-09$06.00

therein). This task is reasonably simple if several derivatives of good quality are available. However, it is often the case that no independent phase estimation is possible, either because of uneven derivatives or common sites or simply because only one derivative is available.

For these cases, it becomes crucial to break the direct connection between the protein phase and the heavy-atom parameters. To accomplish this task, we will explore the possibility of modifying the phases *via* the introduction of new information about the electron density distribution.

These phase-refinement procedures, which rely on modifying the electron density distribution, can significantly improve the quality of the electron density map (Podjarny, Bhat & Zwick, 1987, and references therein). They have the additional property, crucial in this context, of rendering the set of phases under refinement more independent of heavy-atom parameters.

A heavy-atom refinement based on this concept has been applied with success to solve the structure of the glutaminyl-tRNA synthetase complex (Rould, Perona, Soll & Steitz, 1989; Rould, Perona & Steitz, 1992), where this method proved to be adequate due particularly to the presence of common sites. We have applied the same idea in our laboratory and tested it on previously determined structures. A detailed discussion of the results of this work follows.

Algorithms

Fig. 1 shows a flowchart of the algorithm used in this work. A first set of heavy-atom parameters is obtained from heavy-atom amplitude refinement against centric differences, performed independently for each derivative (*A*). This set of parameters leads to a native MIR phase determination, where only the r.m.s. lack of closure is minimized (*B*). The map obtained from this set of phases is subjected to a density-modification procedure, where solvent flattening is used to improve the quality of the map. This density-modification procedure includes a mask-determination step. It is repeated until the phases do change by less than a preset value and the resulting phases are then used to perform a phase refinement of heavy-atom parameters, where the difference between calculated and observed derivative amplitudes is minimized independently for each derivative (*C*). This new set of parameters is then used to recalculate a set of MIR native phases (*B*), which in turn is used to calculate a map that is subjected to the density-modification procedure. The outer cycle is iterated until the heavy-atom parameters converge.

This procedure has been implemented using programs of the *CCP*4 suite (SERC Daresbury Laboratory, 1986), such as *REFINE*2 for the heavy-atom refinement, *PHARE* for the heavy-atom phasing and *RFACTOR*, *TRUNCMAP*, *ENVELOPE*, *FLATMAP* and *FFT* for the solvent-flattening procedure (Wang, 1985; Leslie, 1988). The weights employed during refinement by the program *REFINE*2 were $1/\sigma^2$ for the centric refinement and m^2 for the phased refinement (where m is the figure of merit).

Test cases

To check whether this procedure acts as a refinement of heavy-atom parameters, several test cases were set up. The results of a calculated case using data from cardiotoxin, a small protein of molecular weight 6715 daltons (Rees, Bilwes, Samama & Moras, 1990),

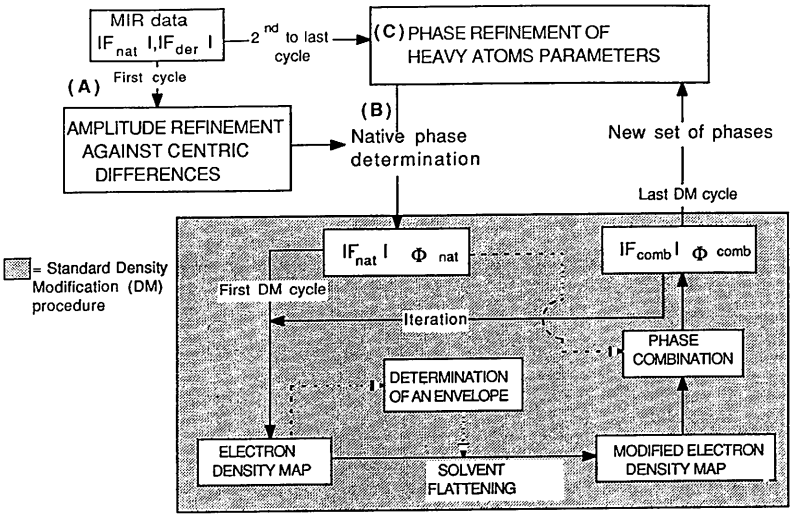

Fig. 1. Flowchart of the proposed algorithm. Details are given in the text. The shaded area corresponds to the density-modification procedure, which is executed once per large cycle. Note that the possibility of combining observed and calculated amplitudes is considered, *e.g.* $F_{comb} = 2F_{obs} - F_{calc}$ might be used as an imput to the next cycle.

and a single derivative have been published elsewhere (Cura *et al.*, 1992) and have proved that the method acts as a refinement procedure. To test whether this method can improve the results obtained from a standard refinement protocol, such as refinement using centric reflections (Dodson, 1976), a second case was studied.

For this test, the data from $tRNA^{Asp}$ crystals at 3 Å resolution were used. tRNA crystallizes in the $C222_1$ space group ($a = 61.5$, $b = 67.5$, $c = 149.5$ Å). The solvent occupies 70% of the volume. The structure was originally solved using two derivatives: Gd (one site) and Au (two sites) (Moras *et al.*, 1980). The Gd derivative is good and the Au derivative shows a strong lack of isomorphism at high resolution. The final R factor was 0.195 at 3 Å resolution (Westhof, Dumas & Moras, 1985).

The observed data were used for both native and derivative amplitudes. The starting positions were those obtained from difference Patterson maps and a refinement of all parameters (native-to-derivative scale, heavy-atom positions, heavy-atom occupancies, heavy-atom temperature factors) was done in separate steps against centric reflections. The positions obtained from this refinement were particularly accurate (within 0.3 Å) for the Gd atom. This is related to the fact that in refinement against centric reflections there is no phase error (with the exception of crossovers) in the calculation of ΔF_{iso} and hence F^{obs}(heavy).

A first trial of cycling density modification and heavy-atom refinement against density-modified phases in the 3-23 Å range showed that the Gd-position error increased (Fig. 2). This is not unexpected, since position refinement against phases that are in error can be worse than refinement against centric reflections, where there is no phase error. Moreover, this could be corrected by limiting the resolution range of the reflections used for position refinement of Gd to 3-7 Å (Fig. 2). This indicates that the first

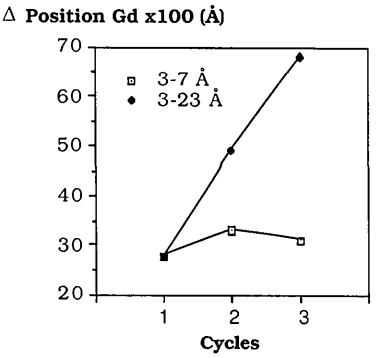

Fig. 2. Positional error of the Gd heavy atom for the tRNA test case during cycles of refinement against density-modified phases. The starting position (point 1) was obtained from refinement against centric reflections. ◆ Using all data between 23 and 3 Å. ⊡ Using data between 7 and 3 Å.

refinement was dominated by strong low-resolution reflections that are not sensitive to positional errors. However, even in these conditions the method did not improve the MIR phases over those obtained using heavy-atom parameters from centric refinement. Therefore, it can be concluded that centric position refinement in a group with three centric projections is accurate and independent of phase errors and cannot be easily improved upon; moreover, at this low level of positional error an improvement will not lead to a large decrease of phase error.

To test worse (and more realistic) initial conditions, a random error of 0.7 Å was imposed on the Gd heavy-atom positions and the refinement against centric reflections between 23 and 3 Å was repeated. This refinement led to a F_{obs} *vs* F_{calc} correlation coefficient of 0.45. The phases obtained from the centric refinement were used as a starting point of a density-modification procedure, using an automatic solvent mask.

The resulting phases were used for a subsequent refinement of heavy-atom parameters. Tests against model phases showed that optimal results are obtained by refining and phasing separately low- and high-resolution reflections. Occupancies and scales obtained from centric refinement are well suited for low-resolution refinement, since centric zones have a larger proportion of low-resolution reflections than noncentric ones. For higher resolution, however, occupancies and scales are refined against density-modified phases, which has the advantage of breaking the dependence of occupancy and scale. The refinement and subsequent phasing were performed separately for two resolution ranges, 23-10 Å and 10-3 Å. Furthermore, positions for the Gd derivative were refined in the 5-3 Å resolution range.

The cycle was iterated four times. Fig. 3 shows the result, in terms of phase error (Fig. 3*a*) and heavy-atom parameters (Figs. 3*b*, *c* and *d*). 'True' values of occupancy and scale have been obtained by refinement against phases calculated from the published model (Westhof, Dumas & Moras, 1985).

The following points should be noted:

(1) The positions converge to the true ones for the Gd derivative and one of the Au positions. The second Au position diverges (this is a very weak site and its error is probably linked to the lack of isomorphism of this derivative).

(2) The native-derivative scale and the occupancies converge for both derivatives to values quite different from those obtained by centric refinement (cycle 1 in Fig. 3) and much closer to the true values (Figs. 3*c* and *d*).

(3) The MIR phases improve by about 2° [Fig. 3(*a*), curve MIR]. The density-modification phases show a similar behavior [Fig. 3(*a*), curve Denmod]. These changes do not have a clearly visible effect on the electron density.

The conclusion of this case, where the initial position accuracy was not very good, is that the method did improve the heavy-atom parameters. In particular, it derived better values of the native-to-derivative scale and the heavy-atom occupancy. In the case of centric refinement, scale and occupancy are strongly correlated and therefore they may both be in error (see Figs. 3*c* and *d*), whereas the present method enables an independent refinement that approaches the correct values. This property can be crucial in cases where exact occupancy values are needed to differentiate derivatives with common sites, as described by Rould, Perona & Steitz (1992).

Analysis of a practical application

This method might be particularly useful for difficult cases where the electron density map is in the limit of interpretability and each additional gain in phase quality is important. This was the case for the aspartyl tRNA synthetase complex from yeast, where it was applied during the solution of the phase problem. The text that follows describes some of the early attempts at the solution of the phase problem that are relevant to this paper and cannot be considered as a full account of the structure solution, which will be published elsewhere.

This complex crystallizes in space group $P2_12_12$, $a = 210.25$, $b = 146.17$, $c = 85.13$ Å, with one synthetase dimer (molecular weight 1.25×10^5 daltons) and two tRNA molecules (molecular weight 0.25×10^5 daltons) per asymmetric unit. The solvent occupies 69% of the volume. At the time of writing, an atomic model is being refined (Ruff *et al.*, 1991). For the purpose of error analysis, a 'current' phase set calculated from this model was used.*

Heavy-atom initial phasing

Data from a native crystal to 2.7 Å and from three heavy-atom derivatives (Hg to 4 Å, Au to 6 Å and Sm to 3.5 Å) were used. Heavy-atom sites were located by difference Patterson maps and cross-difference Fourier maps. Heavy-atom parameters were refined against centric differences between 15 and 5 Å, with statistics of medium quality (Table 1). During the determination of native-derivative scales an algorithm developed by Dumas (1992) based on the statistical considerations was used. These scale factors were kept fixed during the refinement.

* It should be noted that this error analysis differs from a previously published one (Cura *et al.*, 1992) where the phase set available for comparison had been obtained from MIR plus solvent flattening and local symmetry averaging at 3.5 Å resolution.

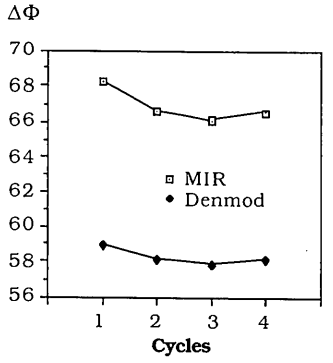

(*a*)

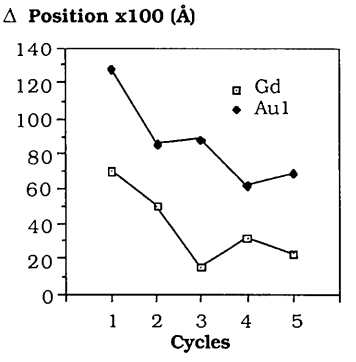

(*b*)

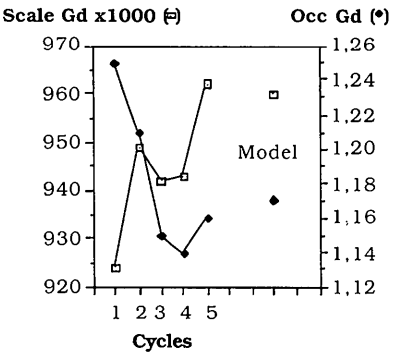

(*c*)

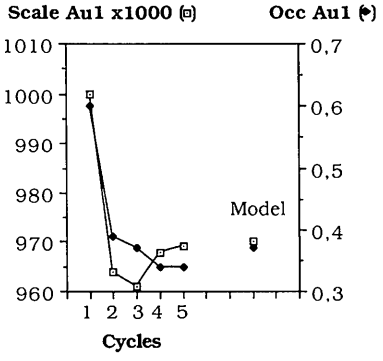

(*d*)

Fig. 3. Evolution of phase error and heavy-atom parameters during the refinement against density-modified phases. The density modification was done using an automatic mask calculated with a solvent content of 50% and an averaging radius of 16 Å and phases with a figure of merit (after phase combination) larger than 0.7 were used in the refinement. These parameters were a result of an optimization process. Four cycles of heavy-atom refinement (the first being against centric reflections), calculation of MIR phases and density modification were performed. The phases obtained from the fourth cycle were used for a fifth refinement after which the process was stopped. (*a*) Mean phase difference with model phases, for phases calculated with *PHARE* (MIR) and after density modification (Denmod). (*b*) Difference in Gd and Au positions. (*c*) Gd occupancy and scale. (*d*) Au occupancy and scale. For (*b*), (*c*) and (*d*), model values are obtained by refinement against model phases.

Table 1. *Centric heavy-atom refinement statistics, for tRNA-synthetase, as obtained from the program REFINE 2*

For a definition of gradient and correlation, see Dodson (1976).

	Hg derivative 15-5 Å, six sites	Au derivative 15-6 Å, two sites	Sm derivative 15-5 Å, two sites
R factor (%)	51	59	66
Gradient (%)	59	31	13
Correlation (%)	51	44	22
Phasing power	2.49	1.74	1.51

These parameters were used to phase 10 562 reflections between 15 and 5 Å, without cutoffs, with an overall FOM of 0.55. The phases derived from the three derivatives were used to calculate a map with terms from 15 to 6 Å. When a refined model became available an analysis was made to assess the quality of these MIR phases. The mean phase error $\langle|\varphi_{MIR}-\varphi_{model}|\rangle$ is 61.5° and the correlation

$$\text{corr}(\rho_1,\rho_2)=\sum[F^2m\cos(\varphi_1-\varphi_2)]/\sum(F^2m)$$

of this map with a similar one calculated with current model phases is 59% [see Figs. 4(*b*) and (*c*), point *A*1, MIR]. Although this map showed regions of connected density it was not clearly interpretable (Figs. 5*a* and 6*a*).

Density modification and heavy-atom iterative refinement

A density-modification procedure by solvent flattening using an automatic mask determination (averaging radius 15 Å, solvent volume 30%) was started. The 6 Å map showed clearly increased contrast that marked the molecular region (Fig. 5*b*). This is linked to a marked decrease of the phase error of the strongest 10% reflections from 46° [Fig. 4(*b*), point *A*1, MIR, large *F*'s] to 36° [Fig. 4(*b*), point *A*1, Denmod, large *F*'s]. However, detailed analysis showed that the continuity had not significantly improved and that large solvent regions had not been identified [labelled *S* in Fig. 5(*b*); see also Fig. 6(*b*)]. Indeed, the correlation of this map with a similar one calculated with current phases is barely higher (60%, Fig. 4*c*) than in the MIR case and the overall phase error is slightly lower (59°, Fig. 4*b*).

At this point, a five-cycle procedure of iterative density modification and heavy-atom refinement (of which the first density modification had already been done) with terms from 15 to 5 Å was engaged, the final map being shown in Fig. 5(*c*). Fig. 4 shows the evolution of the occupancy of the Hg heavy atoms [Fig. 4(*a*), *A* cycles], the phase difference with model phases [Fig. 4(*b*), *A* cycles] and the correlation with a model map [Fig. 4(*c*), *A* cycles]. The final MIR figure of merit is 0.6. It should be noted that the r.m.s.

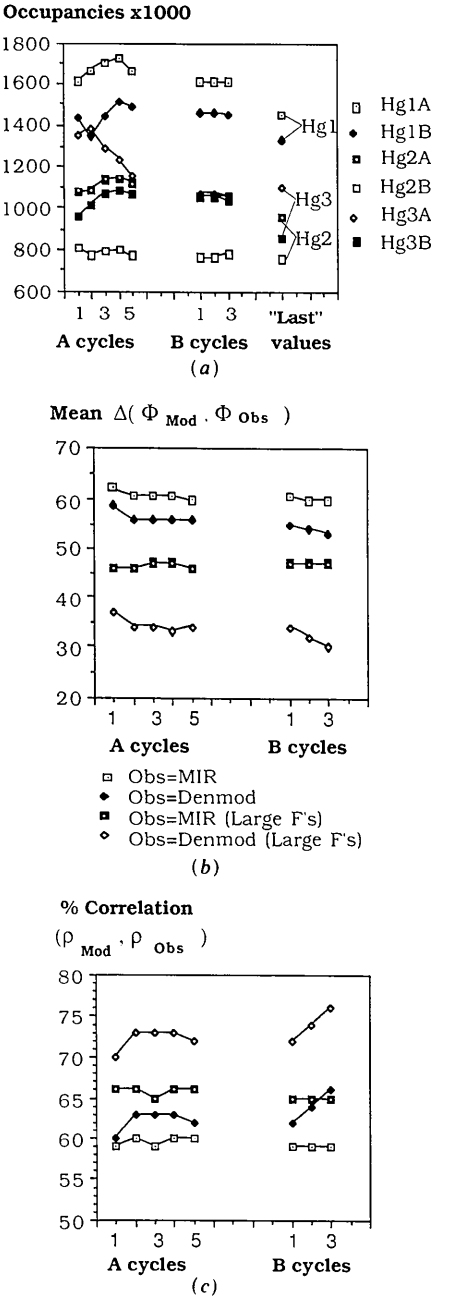

Fig. 4. Evolution of (*a*) Hg occupancy, (*b*) phase error and (*c*) correlation with the correct map during the refinement of heavy-atom parameters for the case of the tRNA synthetase complex. The *A* cycles correspond to the initial cycles with masks computed at 30% solvent. The *B* cycles correspond to the subsequent cycles where the mask parameters were changed (see text). The MIR phases are obtained from *PHARE*. The Denmod phases are obtained after completion of the density-modification procedure. The large *F* phases correspond to the 10% largest amplitudes. The Hg atoms Hg1*A*, Hg2*A* and Hg3*A* are linked to one synthetase monomer. The Hg atoms Hg1*B*, Hg2*B* and Hg3*B* are the corresponding ones related by a local twofold axis. The occupancies shown are those obtained by refinement against Denmod phases. The 'last' values shown are obtained by refinement against the last experimental phases, which are the result of local symmetry averaging and phase extension.

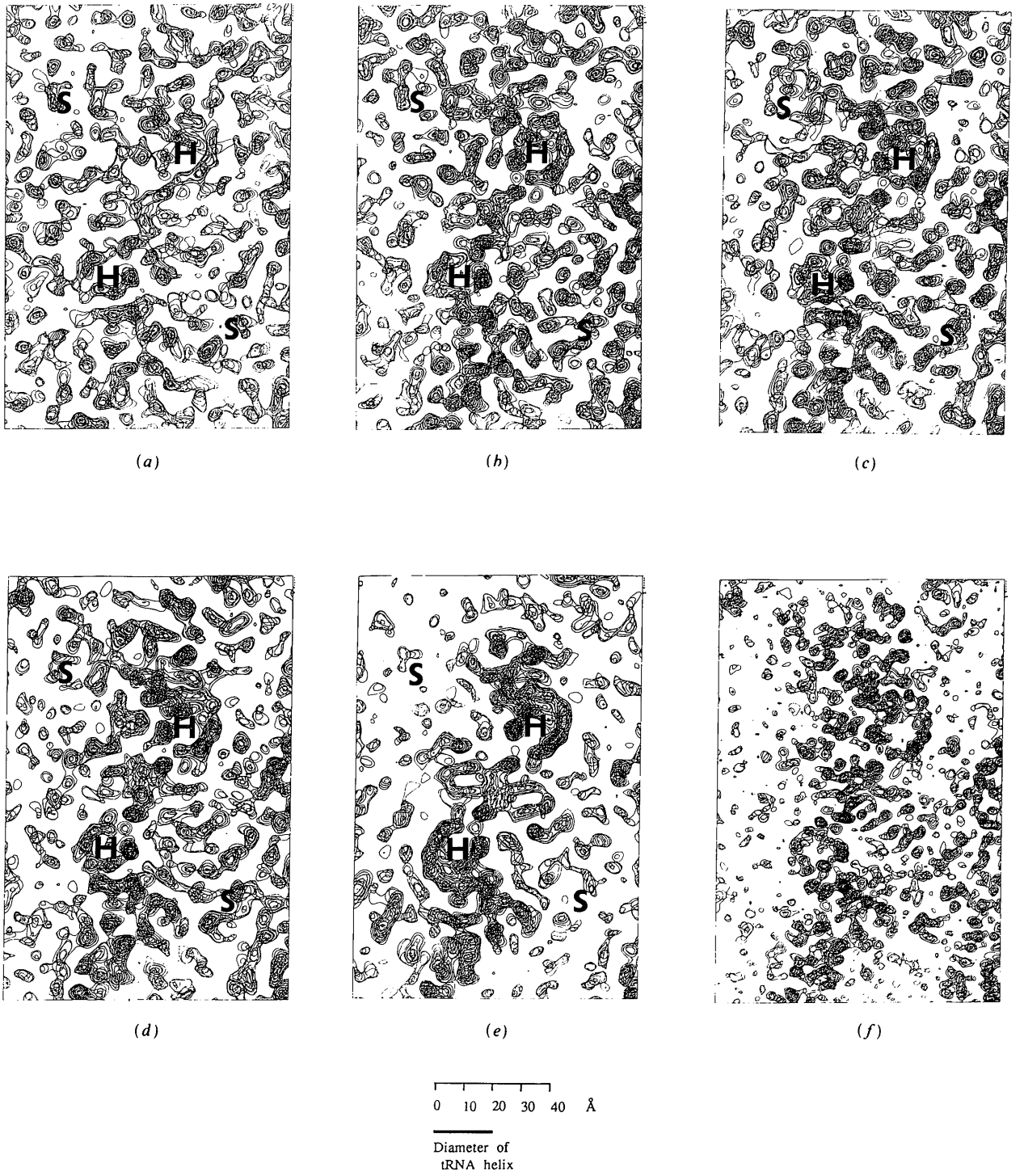

Fig. 5. Electron density maps of the tRNA synthetase complex showing the effect of heavy-atom refinement and mask parameter change. The map is viewed down the local twofold axis, which is at the center of the figure. No averaging is done. The sections shown comprise the acceptor stem helices of the tRNA molecules, indicated by the letter *H*. The letter *S* indicates a solvent zone close to the molecular boundary. (*a*) Initial 6 Å SIR map with heavy-atom parameters from centric refinement. Note the lack of contrast and the poor definition of the helical zones. (*b*) First 6 Å density-modified map. Note the increase in contrast. However, the helical region definition has not increased. (*c*) 6 Å density-modification map after *A* cycles. Small changes, notably a better defined solvent zone. (*d*) 6 Å density-modification map after *B* cycles. Better definition of the helical zones, which approach the shape of the calculated map. (*e*) 6 Å map with calculated model phases. (*f*) 4 Å map obtained following *B* cycles. Much better definition of the helical zones, which show clearly the phosphate positions. Clear solvent zone.

difference between heavy-atom positions linked by the local twofold axis diminished during this procedure from 0.47 to 0.30 Å.

The results so far can be summarized as follows:

(1) One occupancy (Hg3*A*) changed significantly and it approached the value observed in the second monomer (Hg3*B*).

(2) During the cycles, the phase and map quality improved slightly for both the MIR and the Denmod maps [Figs. 4(*b*) and (*c*), *A* cycles]. For example, the correlation of the Denmod maps with the current one improved from 60 to 62% and that of the MIR maps improved from 59 to 60%. The mean error in MIR phases diminished from 61 to 60°. It should be

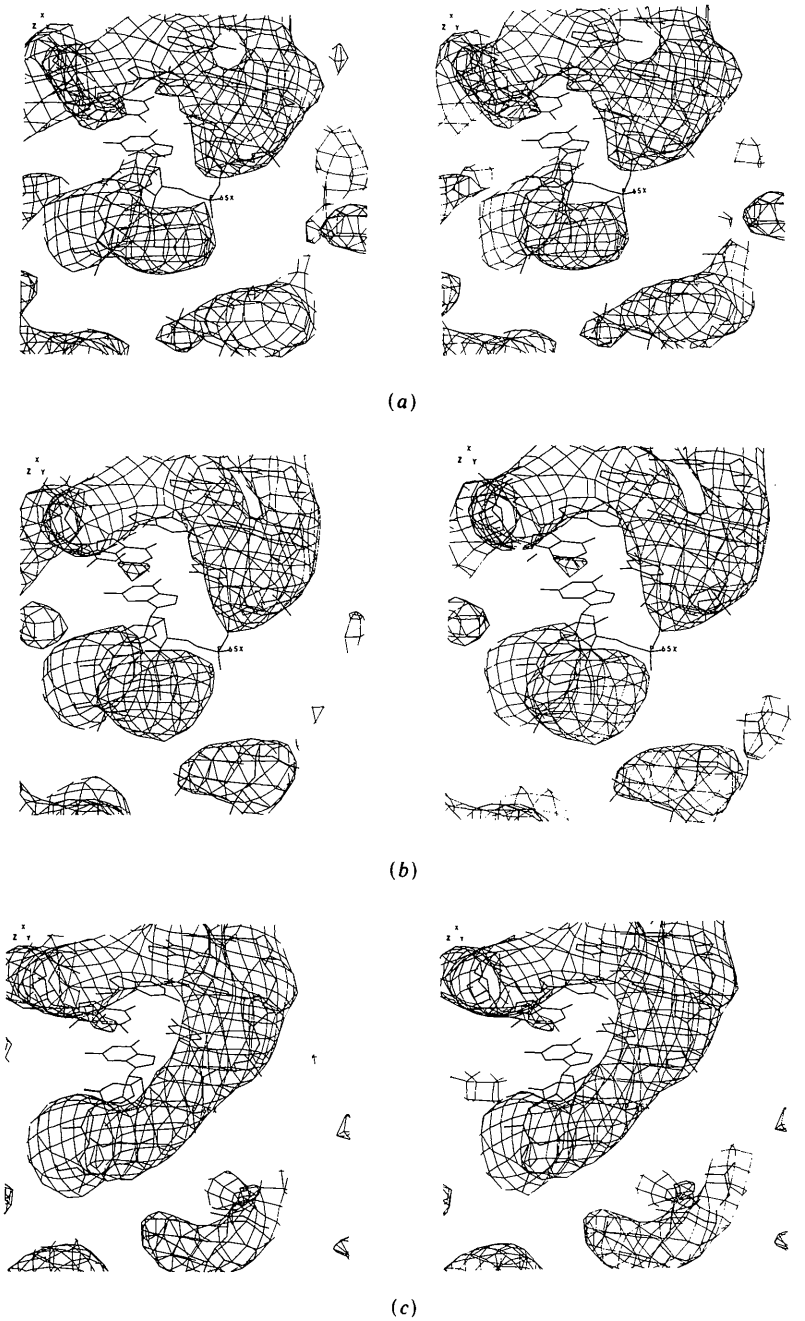

Fig. 6. Local portion of electron density map illustrating the improvement in continuity. (*a*) Initial 6 Å SIR map with heavy-atom parameters from centric refinement. Note the lack of continuity of the helical stem (corresponds to Fig. 5*a*). (*b*) First 6 Å density-modified map. Note that the helical region definition has not improved (corresponds to Fig. 5*b*). (*c*) 6 Å density-modification map after *B* cycles. Good continuity of the helical zones (corresponds to Fig. 5*d*).

noted that this effect finished after the second cycle; afterwards there was either no improvement or even deterioration. For example, the correlation of Denmod maps went through a maximum of 63% and then dropped to 62%.

(3) These effects are amplified if we consider only the 10% largest F's (Figs. 4*b* and *c*). We also see the effect noted before of a larger improvement for these structure factors using density modification.

Even when these improvements are measurable in terms of statistics, the direct effect on map intepretability is very small (Figs. 5*b* and *c*). The most important effect of the improved quality of MIR phases associated with large F's was the calculation of a better mask (Fenderson, Herriott & Adman, 1990). This is shown by the B points of Fig. 4, comprising three additional cycles where the heavy atoms were refined after each density-modification procedure. The mask-defining parameters were made more restrictive as follows:

First cycle: averaging radius 15 Å, solvent volume 30%.

Second cycle: averaging radius 10 Å, solvent volume 40%.

Third cycle: averaging radius 10 Å, solvent volume 45%.

The density-modification procedure gave in this case a map with a correlation of 66% with the current one, showing a clear improvement (Fig. 5*d*). As a comparison, the corresponding map calculated with model phases is shown (Fig. 5*e*). This effect is even more noticeable for the 10% reflections of highest amplitude, where the phase error diminished to 32° (Fig. 4, cycle *B*3). The map was recalculated at 4 Å (Fig. 5*f*). The higher-resolution map, which had a correlation of 54% with the model one and a phase error of 61°, clearly showed the phosphate positions in the tRNA. It is therefore clear that the size of the envelope is a critical parameter to improve the quality of density modification. It should be noted that this analysis is done *a posteriori*; at the time of the structure solution it was not known for certain whether the 45% solvent mask was significantly better than the 30% mask, as is shown above. It should also be noted that the comparison with the current model shows some small regions where the 45% mask cuts the model.

As an illustration of the local effect of this procedure, Fig. 6 shows a portion of the electron density map corresponding to the tRNA stem calculated with three different phase sets. The initial MIR map (Fig. 6*a*) shows a clear chain discontinuity at the level of *P*65. This discontinuity is not solved after the first cycle of density modification (Fig. 6*b*). However, the final 6 Å map after the B cycles outlined above (Fig. 6*c*) clearly shows the continuous chain.

After the procedures described above, new improved rescaled data were used. With these data the procedure was restarted; a heavy-atom refinement was done at 6 Å with the phases obtained previously with the larger mask (point *B*1, 30% solvent content, 15 Å radius). The procedure was continued at 4 Å with a mask defined with a solvent content of 30% and a radius of 10 Å. To ensure that no portion of the model was cut, this mask was then kept fixed throughout the structure solution, which then proceeded to 3.0 Å resolution and a refined model.

Concluding remarks

Additional refinement of heavy-atom parameters increases scale and occupancy accuracy and diminishes phase error. However, the size of this decrease might be too small to be significant and the case is less clear for position refinement, where the result depends on the size of the original error.

Increased phase accuracy, especially of structure factors with large amplitudes, leads to a better molecular envelope and to a more efficient density-modification procedure, which in turn can lead to improved phases at higher resolution.

In this sense, the additional refinement of heavy-atom parameters can and should be considered as part of a larger process where both the heavy-atom parameters and the density-modification parameters are varied.

We thank P. Dumas, D. Moras, B. Rees, J. M. Rondeau, F. Tête-Favier and J. C. Thierry for their continuous support, interest, useful ideas and discussions. We thank M. Rould and T. Steitz for the successful scientific collaboration and interchange of information concerning the method described. We thank A. Urzhumtsev for his careful reading of the manuscript.

References

BLOW, D. M. & CRICK, F. H. C. (1959). *Acta Cryst.* **12**, 794-802.

BLOW, D. M., HENRICK, K. & VRIELINK, A. (1988). *Improving Protein Phases.* Proc. Daresbury Study Weekend, pp. 32-38. SERC Daresbury Laboratory, Warrington, England.

BRICOGNE, G. (1992). *Isomorphous Replacement and Anomalous Scattering.* Proc. Daresbury Study Weekend. SERC Daresbury Laboratory, Warrington, England. In the press.

CURA, V., PODJARNY, A. D., KRISHNASWAMY, S., REES, B., RONDEAU, J. M., TETE, F., MOUREY, L., SAMAMA, J. P. & MORAS, D. (1992). *Isomorphous Replacement and Anomalous Scattering.* Proc. Daresbury Study Weekend. SERC Daresbury Laboratory, Warrington, England. In the press.

DODSON, E. J. (1976). In *Crystallographic Computing Techniques*, edited by F. R. AHMED, pp. 259-268. Copenhagen: Munskgaard.

DUMAS, P. (1992). Submitted to *Acta Cryst.* A.

FENDERSON, F. F., HERRIOTT, J. R. & ADMAN, E. T. (1990). *J. Appl. Cryst.* **23**, 115-131.

LESLIE, A. G. W. (1988). *Improving Protein Phases.* Proc. Daresbury Study Weekend, pp. 25-31. SERC Daresbury Laboratory, Warrington, England.

MORAS, D., COMARMOND, M. B., FISCHER, J., WEISS, R., THIERRY, J. C., EBEL, J. P. & GIEGÉ, R. (1980). *Nature (London)*, **288**, 669-674.

OTWINOWSKI, Z. (1992). *Isomorphous Replacement and Anomalous Scattering.* Proc. Daresbury Study Weekend. SERC Daresbury Laboratory, Warrington, England. In the press.
PHILIPS, S. E. V. (1988). *Improving Protein Phases.* Proc. Daresbury Study Weekend, pp. 1-12. SERC Daresbury Laboratory, Warrington, England.
PODJARNY, A. D., BHAT, T. N. & ZWICK, M. (1987). *Annu. Rev. Biophys. Biophys. Chem.* **16**, 351-373.
READ, R. J. (1991). In *Crystallographic Computing* 5, edited by D. MORAS, A. D. PODJARNY & J. C. THIERRY, pp. 158-168. Oxford Univ. Press.
REES, B., BILWES, A., SAMAMA, J. P. & MORAS, D. (1990). *J. Mol. Biol.* **214**, 281-297.
ROULD, M. A., PERONA, J. J., SOLL, A. & STEITZ, T. A. (1989). *Science* **246**, 1135-1141.
ROULD, M. A., PERONA, J. J. & STEITZ, T. A. (1992). *Acta Cryst.* A**48**, 751-756.
RUFF, M., KRISHNASWAMY, S., BOEGLIN, M., POTERSZMAN, A., MITSCHLER, A., PODJARNY, A., REES, B., THIERRY, J. C. & MORAS, D. (1991). *Science*, **252**, 1682-1689.
SERC Daresbury Laboratory (1986). *CCP4. A Suite of Programs for Protein Crystallography.* SERC Daresbury Laboratory, Warrington, England.
WANG, B. C. (1985). *Methods Enzymol.* **115**, 90-112.
WESTHOF, E., DUMAS, P. & MORAS, D. (1985). *J. Mol. Biol.* **184**, 119-145.

Acta Cryst. (1992). A**48**, 764-771

Evaluation of the Roughness of a Crystal Surface by X-ray Scattering. I. Theoretical Considerations

BY JIMPEI HARADA

Department of Applied Physics, Nagoya University, Chikusa-ku, Nagoya 464-01, *Japan*

(*Received* 18 *November* 1991; *accepted* 16 *March* 1992)

Abstract

The relationship between the intensity distributions of the crystal truncation rod (CTR) scattering and the surface roughness of a crystal is discussed by developing a kinematic theory for the CTR scattering so as to reflect the two-dimensional aspect of the surface. The intensity of the CTR scattering elongated from a Bragg point is shown to be reduced by a factor $|\Gamma(q)|^2$ for a surface possessing some roughness, where $\Gamma(q)$ is defined by a simple Fourier summation of γ_p, the relative area with the same step height p on a surface, *i.e.* $\Gamma(q)=\sum_{p=0}^{\infty}\gamma_p \exp(2\pi ipq)$, with $\sum_p \gamma_p = 1$, q being the distance in reciprocal space from the Bragg point along the CTR scattering. A pair-correlation function between the steps can, therefore, be obtained by a simple Fourier integral of the roughness damping factor $|\Gamma(q)|^2$. For the case where γ_p has a Gaussian distribution around the average step height, $|\Gamma(q)|^2$ is approximated by the well known Debye-Waller-like factor, $\exp(-4\pi^2\langle\Delta p^2\rangle q^2)$, where $\langle\Delta p^2\rangle$ is the mean square deviation of step height in units of the lattice spacing. The intensity formulae proposed so far by several authors are also discussed on the basis of the above factor.

Introduction

The effect on the diffraction pattern of the abrupt truncation of a crystal at the surface is to give rise to rod-shaped scattering elongated from each Bragg point in a direction normal to the crystal surface. The rod-shaped scattering is referred to as crystal truncation rod (CTR) scattering in X-ray diffraction. The intensity distribution along the rod depends very much on the condition of the surface, such as the surface roughness and the surface lattice relaxation. Thus, the analysis of the CTR scattering can provide valuable information on the lattice modulation at a crystal surface and also on the interface boundary on an atomic scale, as demonstrated by several authors. Andrews & Cowley (1985) showed that the intensity of the CTR scattering is proportional to the inverse square of the distance from the Bragg point for the ideally flat surface but falls off from it by a Debye-Waller-like factor for a surface with some roughness. On the other hand, Robinson (1986) showed that surface morphology of an Si(111) surface can be discussed on an atomic scale on the basis of the CTR scattering. Afanas'ev, Aleksandrov, Fanchenko, Chaplanov & Yakimov (1986) and Kashihara, Kawamura, Kashiwagura & Harada (1987) pointed out that it is also possible to evaluate the surface lattice relaxation if, in addition, the asymmetry of the CTR scattering with respect to the Bragg point is taken into account.

In representing the intensity modulation along the CTR scattering due to surface roughness, other theoretical approaches have also been proposed by Vlieg, van der Veen, Gurman, Norris & Macdonald (1989) and Kashihara (1990). However, the extent of the validity for the formulae presented and also their relationships have not so far been clarified. It is, therefore, important to assess the validity of these formulae in order to evaluate the roughness of various

0108-7673/92/050764-08$06.00